



Contents lists available at ScienceDirect

Arabian Journal of Chemistry

journal homepage: [www.sciencedirect.com](http://www.sciencedirect.com)

Original article

# High affinity of protocatechuic acid to human serum albumin and modulatory effects against oxidative stress and inflammation in alveolar epithelial cells: Modulation of pulmonary fibrosis

Chang Liu<sup>a</sup>, Chujie Zhang<sup>a</sup>, Mengqiu Li<sup>a</sup>, Jing Fu<sup>a</sup>, Haichen Yang<sup>a</sup>, Wenhan Ge<sup>a</sup>, Yan Shi<sup>a</sup>, Yang Lee<sup>b</sup>, Cheng Huang<sup>a,\*</sup>

<sup>a</sup> Department of Emergency Center, Affiliated Huaian Hospital of Xuzhou Medical University, Huaian 223002, China

<sup>b</sup> Nanjing First Hospital, Nanjing Medical University, Nanjing, Jiangsu Province, China

## ARTICLE INFO

## Article history:

Received 19 March 2023

Accepted 30 August 2023

Available online 4 September 2023

## Keywords:

Human serum albumin

Protocatechuic acid

Interaction

Antioxidant

## ABSTRACT

Protocatechuic acid (PCA), C<sub>7</sub>H<sub>6</sub>O<sub>4</sub>, has been shown to possess potential antioxidant properties. But its interaction with the main plasma carrier protein, human serum albumin (HSA), as well as its antioxidant mechanism remains largely unknown. It has been shown that induced pulmonary fibrosis can be modulated through mitigating epithelial apoptosis mediated by the prohibition of oxidative stress. Therefore, in this study, the interaction of PCA and HSA was explored by spectroscopy, calorimetry (DSC), as well as molecular docking studies. Also, the protective effects of PCA against lipopolysaccharide (LPS)-induced cytotoxicity and oxidative stress were evaluated by MTT, ROS, ELISA, real-time PCR, and western blot assays. It was shown that under the interaction of HSA with PCA a spontaneous interaction occurs with the contribution of hydrophobic forces, which results in the formation of a stable complex. Cellular assays showed that PCA reduced LPS-induced cytotoxicity in human type II alveolar epithelial cells (AECs) through mitigation of ROS production, release and gene expression of TNF- $\alpha$  and IL-1 $\beta$  as pro-inflammatory mediators, and caspase-3 gene and protein as an apoptotic factor. Also, it was shown that PCA can reduce the expression of NF- $\kappa$ B at the protein level, indicating a possible inhibition of pulmonary fibrosis via regulating the NF- $\kappa$ B signaling pathway. In conclusion, PCA could be a promising therapeutic agent for the control of oxidative stress in AECs which is an important factor in redox modulatory therapy, while its pharmacodynamics can be modulated by interaction with HSA.

© 2023 Published by Elsevier B.V. on behalf of King Saud University. This is an open access article under the CC BY-NC-ND license (<http://creativecommons.org/licenses/by-nc-nd/4.0/>).

## 1. Introduction

Human serum albumin (HSA) is known as a crucial carrier macromolecule for a number of endogenous and exogenous ligands (Forsthuber et al. 2020). In fact, HSA can interact with a wide variety of therapeutic compounds and regulate their pharmacodynamics (Kratz et al. 2014). Exploring the interaction of bioactive compounds with HSA can reveal the characteristics of drug-HSA complexes, as it may furnish important details regarding the

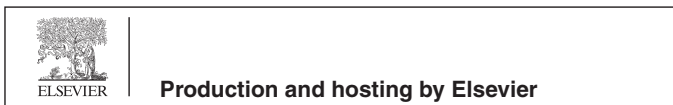
structural properties that influence the therapeutic potency of bioactive compounds especially those derived from medicinal plants (Merlino et al. 2023). Interaction with carrier proteins such as HSA could provide useful information about understanding the toxicity of therapeutic agents and the corresponding biodistribution (Varshney et al. 2010; Yu et al. 2022). Therefore, the investigation of the interaction between bioactive molecules and HSA has been a potential research area in different fields, such as life science, biochemistry, and even medicine (Siddiqui et al. 2021).

Promising advancements are becoming apparent in the application of bioactive compounds-derived pharmaceuticals. The various applications of bioactive compounds from plant materials in medicine, such as antioxidant, anticancer, and antibacterial properties, have been investigated over the past few years (Parham et al. 2020; Vuong et al. 2021; Nwozo et al. 2023). Recent research in this field has focused on the use of protocatechuic acid (PCA), C<sub>7</sub>H<sub>6</sub>O<sub>4</sub>, with a molar mass of 154.12 g/mol and a density of 1.54 g/cm<sup>3</sup> serves as a potential therapeutic compound (Mert

\* Corresponding authors.

E-mail address: [18762043161@163.com](mailto:18762043161@163.com) (C. Huang).

Peer review under responsibility of King Saud University.



et al. 2023; Zhou et al. 2023). PCA as a dihydroxybenzoic acid belonging to the family of phenolic acid structures, can be used as a potential antioxidant compound with minor serious side effects in the biological system (Khan et al. 2022; Liang et al. 2022; Zhou et al. 2023; Jiang et al. 2023). This potential small molecule then enables us to develop promising platforms against side effects induced by oxidative stress.

Chronic obstructive pulmonary disease (COPD) is a chronic respiratory disorder with systemic symptoms that markedly influence the quality of life of patients, which is linked with airflow obstruction along with lung inflammation and destruction (Stolz et al. 2022). COPD is normally a disease during the aging process and oxidative stress markers and reactive oxygen species (ROS) can alter biological molecules, signaling pathways and molecular functions of antioxidants, which heavily contribute to the pathogenesis of COPD (Dailah et al. 2022). The function of several related cells in COPD patients is changed in the course of this disorder, and the expression of crucial oxidant and antioxidant molecules may be dysregulated (Barnes et al. 2022). Therapeutic compounds such as small molecules may restore the balance of ROS production and affect some aspects of this disease (Dailah et al. 2022).

Although some findings recommend that PCA could be utilized as a therapeutic agent for chronic disease induced by oxidative stress (Abdelrahman et al. 2022; Lee et al. 2022; Kassab et al. 2022), further investigations associated with humans are required. Also, the interaction of PCA and HSA can provide useful information about the regulation of this bioactive molecule in the biological system and its biodistribution.

## 2. Materials and methods

### 2.1. Materials and solution preparation

The human pulmonary alveolar epithelial cells (AECs) were obtained from the American Type Culture Collection (ATCC; Manassas, VA, USA). Human serum albumin and protocatechuic acid were purchased from Sigma-Aldrich Co. (USA). The HSA was dissolved in Tris-HCl buffer solution (50 mM Tris, 150 mM NaCl, pH 7.4). For protein and cellular assays, protocatechuic acid was dissolved in Tris-HCl buffer solution or cell culture medium, respectively.

### 2.2. Fluorescence emission spectroscopic study

By fixing the excitation wavelength (280 nm), HSA (2  $\mu$ M) emission intensity under addition of increasing concentrations of PCA from 1 to 30  $\mu$ M was read between 300 and 440 nm at three distinct temperatures of 298/305, 310 K using a Hitachi fluorescence spectrophotometer F-4600 (Tokyo, Japan). The slit widths for both excitation and emission wavelength were set at 5 nm. The data was then used to determine quenching mechanisms as well as binding and parameter constants. The inner filter effect was also considered for the analysis of fluorescence data based on the previous study (Yegoni et al. 2022).

### 2.3. Circular dichroism (CD) study

Alteration of secondary structures of HSA (5  $\mu$ M) under the addition of a concentration of PCA (30  $\mu$ M) at room temperature was determined using a CD spectropolarimeter (JASCO, J-815, Tokyo, Japan). CD spectra were read in 200–260 nm ranges with a scan rate of 100 nm/min and cell length of 0.2 cm.

### 2.4. Differential scanning calorimetry (DSC) analysis

DSC melting analysis was done employing a VP-DSC microcalorimeter (Micro Cal, Northampton, MA) with a heating rate of 1  $^{\circ}$ C/min, over the temperature range from 30 to 100  $^{\circ}$ C. The DSC analyses of HSA (10  $\mu$ M) in the presence of 30  $\mu$ M of PCA were carried out and data was processed with the VP-DSC microcalorimeter software to determine the melting temperature ( $T_m$ ). The DSC analysis was then done based on the previous study (Eskew et al. 2021).

### 2.5. Molecular docking analysis

A molecular docking study was carried out with Autodock Vina software. Compound-free HSA (PDB id: 1AO6) was downloaded from the protein data bank (<https://www.rcsb.org/structure/1ao6>), whereas PCA (PubChem CID: 528594) was downloaded from the PubChem database ([https://pubchem.ncbi.nlm.nih.gov/compound/Protocatechuic-acid\\_-TBDMS](https://pubchem.ncbi.nlm.nih.gov/compound/Protocatechuic-acid_-TBDMS)). The docking format HSA-PCA complex was then determined using AutoDockTools. Docking analysis was done by using a box size of 126  $\text{Å} \times 126 \text{Å} \times 126 \text{Å}$  with a grid size of 0.375  $\text{Å}$ . Si atoms were removed from the PCA compound to perform a docking analysis. From the different complexes deduced from docking, only the complex with the least energy was used for analysis based on a previous study (Faridbod et al. 2011).

### 2.6. Cell culture

AECs were cultured in RPMI 1640 medium containing fetal bovine serum (10%) and antibiotics (1%) incubated in 5%  $\text{CO}_2$  at 37  $^{\circ}$ C. 10  $\mu$ g/ml LPS and 20  $\mu$ M PCA for 24 h were used for induction of oxidative stress and protective effect against cytotoxicity, respectively. This data was fixed at our lab and used for further studies. Therefore, for LPS and PCA incubation, the cells were divided into 3 groups. Group (1): Control AECs with no treatment. Group (2): AECs were only incubated with 10  $\mu$ g/mL LPS for 24 h. Group (3): AECs were incubated with LPS and 20  $\mu$ M PCA for 24 h. After the incubation time, AECs were harvested and used for further assays.

### 2.7. MTT assay

Cell cytotoxicity assay was done using conventional MTT assay. In brief, the AECs were cultured onto 96-well plates overnight. The cells were then incubated as explained in section 2.6 for 24 h. Afterward, the cells were added by 10  $\mu$ L MTT solution at 37  $^{\circ}$ C for 4 h, replaced by 100  $\mu$ L DMSO solution and incubated for 15 min. Finally, the absorbance of each well was detected at 570 nm using an ELISA plate reader (RT-2100C Microplate Reader, China).

### 2.8. Intracellular ROS production assay

DCFDA /  $\text{H}_2$ DCFDA - Cellular ROS Assay Kit (ab113851) was used to assess the generation of ROS based on the provided protocols. Briefly, the cells were seeded and after 24 h, the cells were treated for an additional 24 h. Then, the medium was removed and 100  $\mu$ L DCFDA probe was added to the cells and kept at 37  $^{\circ}$ C for 30 min. The fluorescence intensity of samples was read with Ex/Em at 485/528 nm using a fluorescence microplate reader (Bio-Tek Instruments, Winooski, USA).

## 2.9. ELISA assay

The relative levels of TNF- $\alpha$  and IL-1 $\beta$  in the cell culture supernatant were determined using commercial ELISA kits from Abcam Co. [Human TNF- $\alpha$  ELISA Kit (ab181421)] and [Human IL-1 $\beta$  ELISA Kit (ab214025)], following manufacturer's instructions.

## 2.10. Real-time PCR analysis

The mRNA expression of IL-1 $\beta$ , TNF- $\alpha$ , and caspase-3 was assessed by real-time PCR based on the procedure reported in the previous study (Ileriturk et al. 2022). Briefly, total RNA was isolated using Trizol Lysis Reagent (Invitrogen, China) and complementary DNA (cDNA) synthesis was performed using cDNA Reverse Transcription Kit (Qiagen GmbH, Hilden, Germany). The samples were mixed with SYBR Green PCR Master Mix (Qiagen GmbH, Hilden, Germany) and then assessed on the Applied Biosystems 7500 real-time PCR device.  $\beta$ -actin expression level was used as an internal control, and relative folds determination was done with the  $CT^{-\Delta\Delta CT}$  method.

## 2.11. Western blotting analysis

Western blot analysis was performed similar to the study reported by Yesildag et al. 2022 and Ileriturk et al. 2022. Briefly, 30  $\mu$ g protein from lysed cells were loaded on a 10% sodium dodecyl sulfate-polyacrylamide gel electrophoresis, followed by transferring to the membrane and incubating in 5% BSA, and washing with Tris-buffer saline containing 0.1% Tween 20 after 1 h. The membrane was added to NF- $\kappa$ B, caspase-3, and  $\beta$ -actin primary antibodies (Santa Cruz Biotechnology, Inc., TX) and incubated overnight at 4  $^{\circ}$ C, followed by washing for 5 min. Goat anti-mouse (1:2000) as a secondary antibody was incubated with IgG-HRP for 2 h at room temperature and then washed. Protein bands were detected using enhanced chemiluminescence.

## 2.12. Statistical analysis

The data were expressed as mean  $\pm$  SD of three experiments, and one-way ANOVA, followed by Tukey's post hoc test, was utilized to analyze the data. Statistical difference was reported as significant when  $P < 0.05$ .

## 3. Results and discussion

### 3.1. Effect of protocatechuic acid (PCA) on HSA fluorescence spectra

A number of molecular interactions between ligands and proteins can result in fluorescence quenching of receptors, such as reaction in the excited state, rearrangement at the molecular level, and complex formation (Sarzehi et al. 2010; Khashkhashi-Moghadam et al. 2022; Siddiqui et al. 2021). The quenching mechanisms are mostly categorized as either dynamic or static quenching, which are classified by their varying behaviors against temperature and viscosity (Bose et al. 2016; Mostafavi et al. 2022; Siddiqui et al. 2021). In this assay, the concentration of HSA was fixed at 2  $\mu$ M, and the concentrations of PCA were in the range of 1 to 30  $\mu$ M. The impact of PCA on HSA fluorescence emission intensity at 298 K is displayed in Fig. 1.

It was deduced from Fig. 1 that a progressive quenching in the fluorescence emission intensity was triggered by PCA, associated with a blue shift in wavelength emission maximum ( $\lambda_{max}$ ) in the HSA spectra. This data proposes an enhanced hydrophobicity of the environment around the tryptophan residue (Trp-214).

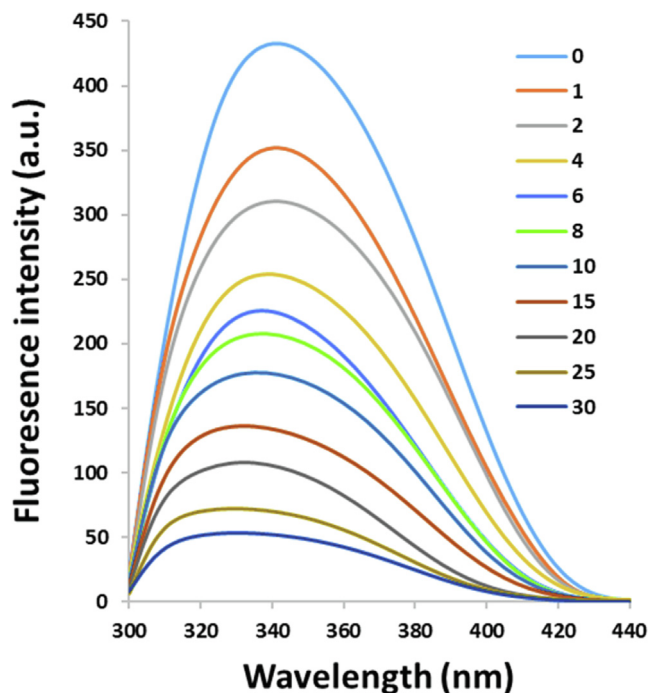


Fig. 1. Fluorescence quenching of HSA (2  $\mu$ M) under the interaction with PCA with increasing concentrations (1–30  $\mu$ M) at room temperature.

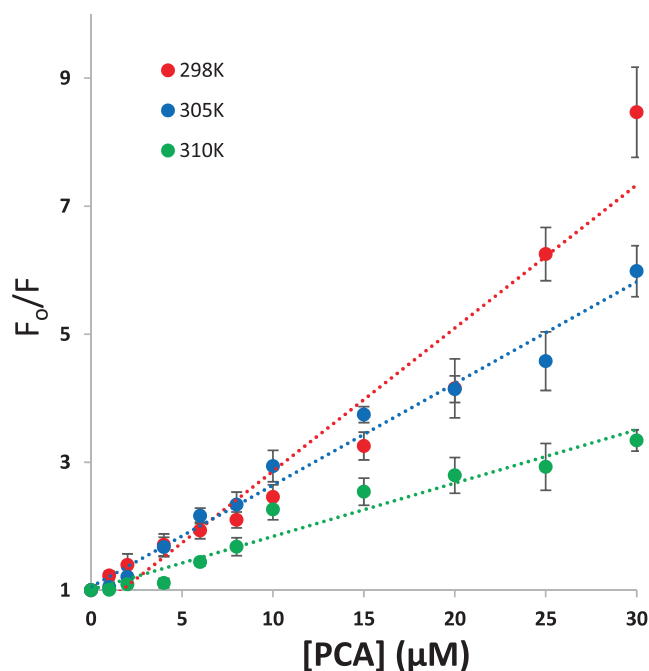


Fig. 2. Stern-Volmer plots for the interaction of PCA and HSA at temperatures of 298 K, 305 K, and 310 K for the calculation of quenching constants.

### 3.2. Effect of protocatechuic acid (PCA) on HSA fluorescence quenching

The quenching parameters were calculated using the Stern-Volmer equation (Farajzadeh-Dehkordi et al. 2023):

$$F_0/F = 1 + K_{SV}[PCA] = 1 + k_q\tau_0[PCA] \quad (1)$$

where  $F_0$  and  $F$  are the fluorescence intensities without and with quencher (PCA), respectively,  $K_{SV}$  denotes the Stern-Volmer quench-

ing constant, [PCA] is the concentration of PCA,  $k_q$  is the quenching rate constant of biomacromolecule, and  $\tau_0$  is known as the average lifetime of the biomacromolecule which is around  $10^{-8}$  s.

The Stern-Volmer plots are exhibited in Fig. 2. It was shown that under the studied concentration range, the data is well-fitted with the Stern-Volmer equation. The determination of  $K_{SV}$  values from Stern-Volmer plots were summarized in Table 1. Based on the effect of PCA on fluorescence quenching at each studied temperature (Fig. 2), the data reveals that the  $K_{SV}$  values are inversely related to temperature, indicating a possible quenching mechanism of PCA-HSA interaction by static complex formation. Also,  $k_q$  values were  $2.23 \times 10^{13} \text{ M}^{-1} \text{ s}^{-1}$ ,  $6.47 \times 10^{13} \text{ M}^{-1} \text{ s}^{-1}$ , and  $0.83 \times 10^{13} \text{ M}^{-1} \text{ s}^{-1}$  at 298 K, 305 K, and 310 K, which were much greater than  $k_q$  values reported for dynamic quenching ( $10^{10} \text{ M}^{-1} \text{ s}^{-1}$ ) (Siddiqui et al. 2021).

### 3.3. Calculation of binding parameters

When ligands interact with a set of equivalent sites on a protein, the binding parameters, including binding constant ( $K_b$ ) and the numbers of binding sites ( $n$ ) can be estimated based on the modified Stern-Volmer equation (Osman et al. 2023):

$$\text{Log } F_0 - F/F = n \log[\text{PCA}] + \log K_b \quad (2)$$

For the system of PCA and HSA, the  $K_b$  and  $n$  values at temperatures of 298 K, 305 K, and 310 K were determined based on Fig. 3 and the resultant data were summarized in Table 1. The  $n$  value was around 1, which suggested that there can be one class of binding sites on HSA for PCA. Also, it was revealed that the  $K_b$  and  $n$  values are directly correlated with temperature, as the higher temperature, the binding parameters increase, furnishing a basis for conformational rearrangement of HSA and more favorable interaction with PCA at higher temperature than that in lower ones (Siddiqui et al. 2021). Based on the  $\log K_b$  values it can be revealed that the magnitude of  $K_b$  values can be in the range of  $10^5$ - $10^7$ , revealing a strong interaction between PCA and HSA. Therefore, it may be suggested that interaction of interaction between PCA and HSA may occur *in vivo* and PCA probably binds to HSA with a great affinity (Chamani et al. 2005).

### 3.4. Calculation of thermodynamic parameters

The binding mode between PCA and HSA can be determined through the evaluation of thermodynamic parameters (Siddiqui et al. 2021). The interaction bonds between ligands and proteins are electrostatic, hydrogen bonds, van der Waals, and hydrophobic forces. To investigate the interaction between PCA and HSA, the thermodynamic parameters were estimated by using the van't Hoff plot (Kabir et al. 2023):

$$\ln K_b = -\Delta H^\circ / RT + \Delta S^\circ / R \quad (3)$$

Where,  $K_b$  is the binding constant,  $\Delta H$  and  $\Delta S$  are the enthalpy and entropy changes, respectively, and  $R$  is the gas constant. If the variation in  $\Delta H$  is not significant under the temperature range of 298 K-310 K, the  $\Delta H$  and  $\Delta S$  can be calculated from the slope

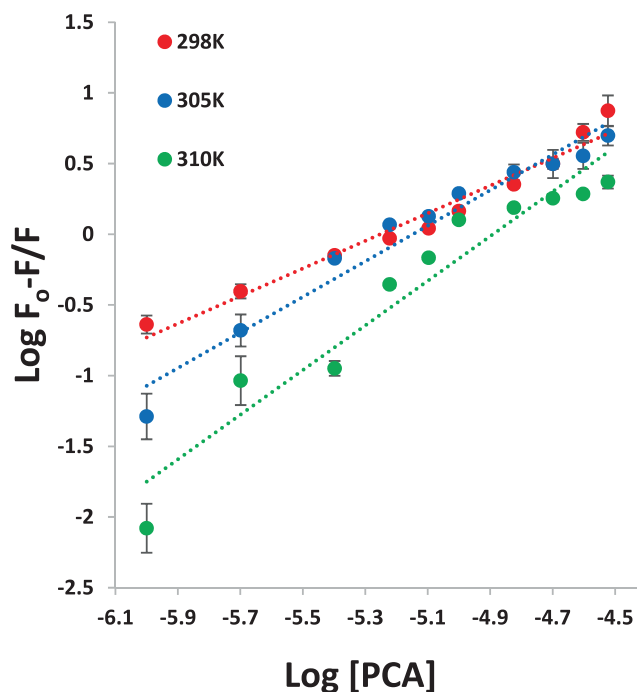


Fig. 3. Modified Stern-Volmer plots for the interaction of PCA and HSA at temperatures of 298 K, 305 K, and 310 K for calculation of binding constants.

and Y-intercept of van't Hoff equation (3), respectively (Fig. 4, Table 1). The free energy change ( $\Delta G$ ) can then be calculated based on the following relationship (Wang et al. 2022):

$$\Delta G = \Delta H - T\Delta S = -RT \ln K_b \quad (4)$$

Table 1 tabulates the  $\Delta H$  and  $\Delta S$  values estimated for the interaction of PCA and HSA. The negative  $\Delta G$  values of  $-29.12 \pm 2.34$  kJ/mol,  $-37.67 \pm 2.93$  kJ/mol, and  $-45.68 \pm 3.68$  kJ/mol at temperatures of 298 K, 305 K, and 310 K, summarized in Table 1, indicated the fact that the interaction system is spontaneous. The  $\Delta H$  value of  $378.65 \pm 23.21$  kJ/mol and  $T\Delta S$  value of  $407.78 \pm 31.24$  kJ/mol indicated that hydrophobic forces are mainly responsible for the interaction of PCA-HSA complex (Siddiqui et al. 2021), which needs docking studies.

### 3.5. Circular dichroism spectra

To obtain information about the secondary structural changes of HSA, Far-UV CD analysis was done at 298 K. The 1:15 M ratio of HSA to PCA was used and the far-UV CD spectra of HSA in the absence (line blue) and presence (line green) of PCA were shown in Fig. 5. Two negative bands were observed in the far-UV region centered at 208 and 222 nm, revealing the dominance of  $\alpha$ -helical structure of HSA due to  $\pi \rightarrow \pi^*$  and  $n \rightarrow \pi^*$  transfer in peptide bonds (Negrea et al. 2023). With the titration of PCA, the band intensity of minima increased in the CD spectrum relative to the control sample. The CD outcomes were analyzed in terms of mean

**Table 1**  
Calculation of different parameters under the interaction of PCA and HSA at temperatures of 298 K, 305 K, and 310 K.

T (K)	$K_{sv}$ ( $10^5 \text{ M}^{-1}$ )	$k_q$ ( $10^{13} \text{ M}^{-1} \text{ s}^{-1}$ )	$\log K_b$	$n$	$\Delta H$ (kJ/mol)	$T\Delta S$ (kJ/mol)	$\Delta G$ (kJ/mol)
298	$2.23 \pm 0.26$	$2.23 \pm 0.26$	$5.12 \pm 0.21$	$0.97 \pm 0.07$	$378.65 \pm 23.21$	$407.78 \pm 31.24$	$-29.12 \pm 2.34$
305	$1.58 \pm 0.12$	$1.58 \pm 0.12$	$6.47 \pm 0.27$	$1.25 \pm 0.09$	$378.65 \pm 23.21$	$416.32 \pm 31.37$	$-37.67 \pm 2.93$
310	$0.83 \pm 0.07$	$0.83 \pm 0.07$	$7.72 \pm 0.35$	$1.57 \pm 0.09$	$378.65 \pm 23.21$	$424.34 \pm 31.39$	$-45.68 \pm 3.68$

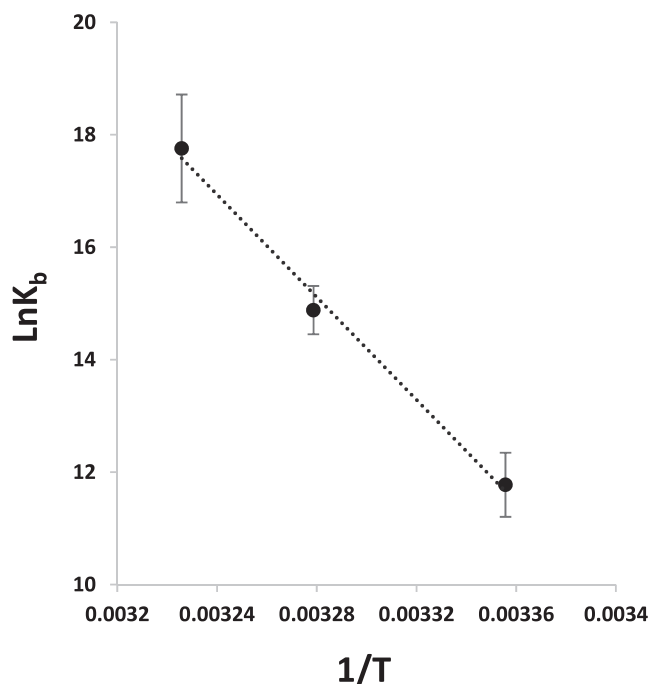


Fig. 4. van't Hoff plot for the interaction of PCA and HSA at temperatures of 298 K, 305 K, and 310 K for calculation of binding constants.

residue ellipticity (MRE) in degree cm<sup>2</sup> dmol<sup>-1</sup> based on the following equation (Rao et al. 2020):

$$MRE = \text{Observed CD}(\text{deg})/C_p n l \times 10 \quad (5)$$

where  $C_p$ ,  $n$ , and  $l$  are the protein concentration, number of amino acid residues, and path length. The  $\alpha$ -helix content of HSA was then estimated from  $MRE_{208 \text{ nm}}$  based on the following equation (Rao et al. 2020):

$$\alpha\text{-Helical}(\%) = -MRE_{208} - 4,000/33,000 - 4,000 \times 100 \quad (6)$$

According to the equations (5) and (6), the  $\alpha$ -helix content of HSA was calculated. This content increased from 58.09% for HSA to 61.39% under the addition of PCA to HSA. The increase of  $\alpha$ -helix structure revealed that PCA combined with several residues of the polypeptide chain and stabilized their hydrophobic and hydrogen bonds (Song et al. 2021). Generally, the incubation of HSA with PCA resulted in a partial increase in minima, while the position of the minima almost kept unchanged, indicating that the interaction of PCA and HSA triggered some secondary structural changes in HSA, where the  $\alpha$ -helical content of HSA elevated.

Therefore, upon interaction of PCA with HSA, the stability of this chiral protein can be increased which can improve the potential application of HSA in different areas (Allenmark et al. 1984).

### 3.6. Thermo stability analysis of PCA–HSA interaction by DSC

Normally, ligand interaction results in either stabilization or destabilization of the proteins (Abarova et al. 2021; Aricov et al. 2020; Rizzuti et al. 2019). DSC analysis was utilized to explore the impact of PCA on the thermal behavior of HSA.  $T_m$  is the main parameter determined from the DSC spectrum that gives detail regarding the impact of ligand interaction on the thermal stability of a biomacromolecule (Naik et al. 2022). Fig. 6 exhibits the DSC thermograms for free HSA and interacted HSA with PCA. It was found that HSA is unfolded in a cooperative manner and gives rise to the formation of an endothermic peak with a  $T_m$  value of around

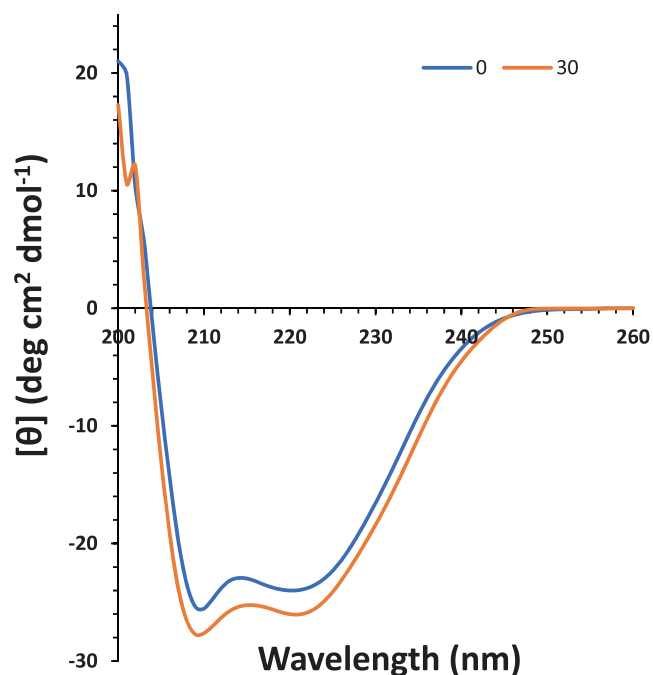


Fig. 5. Far-UV CD study for the interaction of PCA (30  $\mu\text{M}$ ) and HSA (5  $\mu\text{M}$ ) at temperatures of 298 K for exploring the secondary structural changes of the protein.

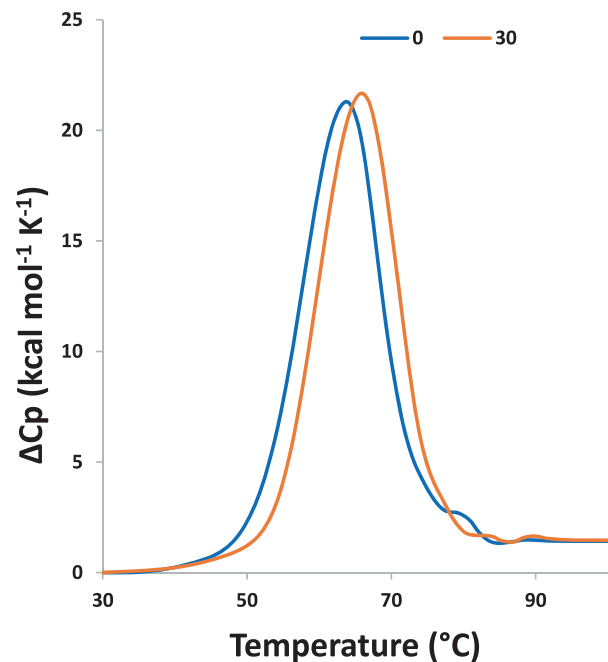
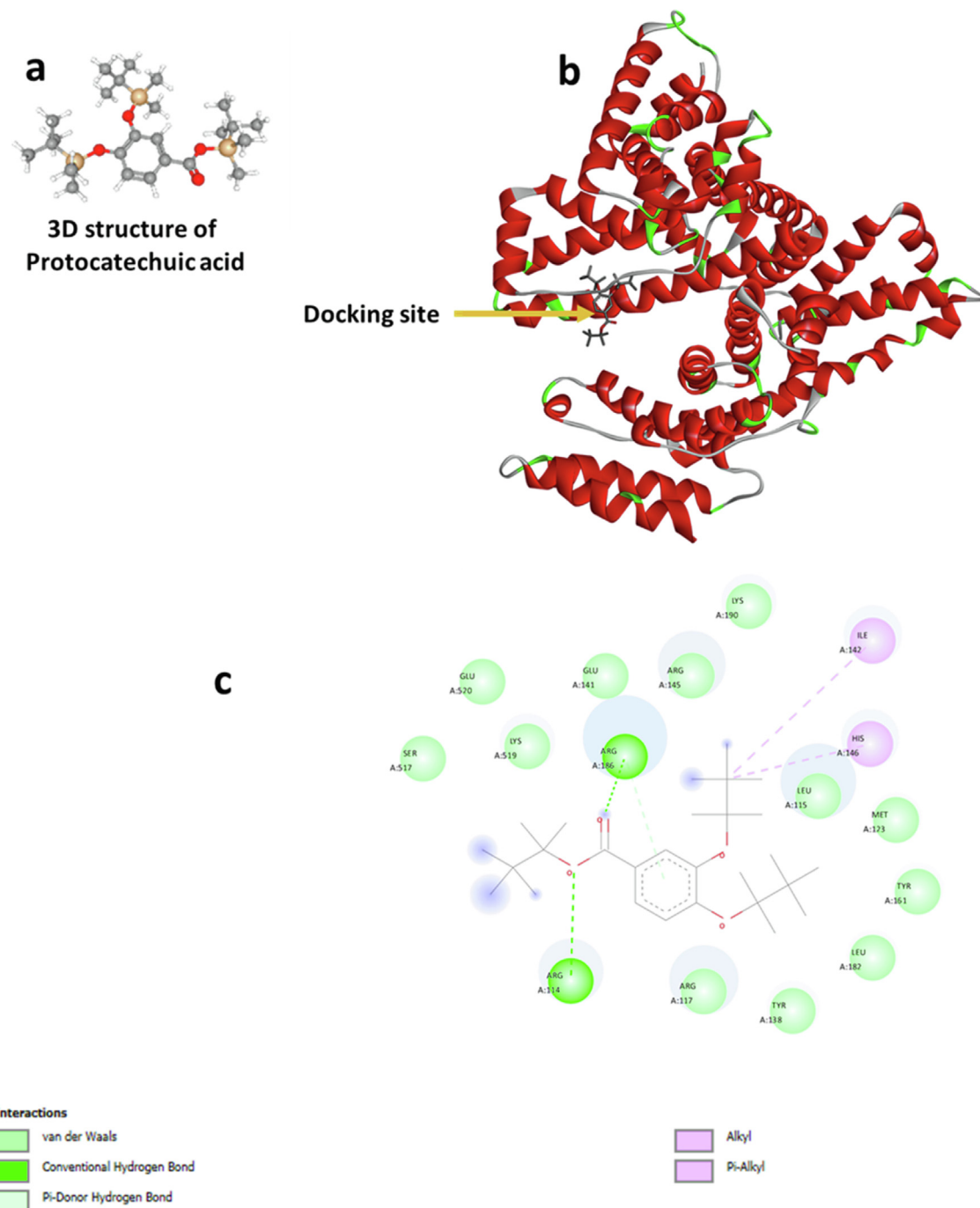


Fig. 6. DSC thermogram for the interaction of PCA (30  $\mu\text{M}$ ) and HSA (10  $\mu\text{M}$ ) for exploring the  $T_m$  of protein.

64 °C (337 K). It was observed that under the interaction of PCA, this ligand could lead to partial stabilization of HSA as supported by the elevation in  $T_m$  by about 2.0 °C. These findings suggested that the interaction of PCA causes stabilization of the HSA structure as also displayed with the CD data. In fact, the increase in the amount of  $\alpha$ -helix content can be a possible reason for increasing the stability and  $T_m$  of protein in the presence of PCA.



**Fig. 7.** Molecular docking study of PCA interaction with HSA. (a) The 3D structure of PCA, (b) docking of HSA and PCA, and (c) the amino acid residues involved in the binding site.

### 3.7. Molecular docking study

The molecular docking study was performed to determine the binding affinity and amino acid residues involved in the interaction of HSA and PCA. Thermodynamic analysis indicated that hydrophobic interactions are the main forces rather than the hydrophilic forces in the formation of HSA-PCA complexes. A rational reason is that dimethyl leads to an enhancement in hydrophobicity of PCA, and strengthens the hydrophobic forces. Generally, PCA molecule (Fig. 7a) after docking analysis (Fig. 7b) existed in a cavity formed by Ile 142 and His 146 (Fig. 7c), which provides a hydrophobic pocket to form alkyl and pi-alkyl interactions with HSA. It was also important to indi-

cate that several other amino acid residues such as Lys 190, Lys 519, Arg 114, Arg 117, Arg 145, Arg 186, Glu 141, Glu 520, Ser 517, Tyr 138, Leu 115, Leu182, Tyr 161, and Met 123 were located in the vicinity of PCA, suggesting that hydrogen bonding interactions also present in the binding site.

### 3.8. PCA mitigated LPS-induced cytotoxicity and ROS production in AECs

The cells were incubated with LPS (10  $\mu\text{g/ml}$ ) for 24 h and it was realized that the cell viability was reduced to around  $46.77\pm 9.47\%$  ( $***P < 0.001$ ) (Fig. 8a), which was in good agreement with a previous study (Jiang et al. 2020). However, co-incubation of AECs with

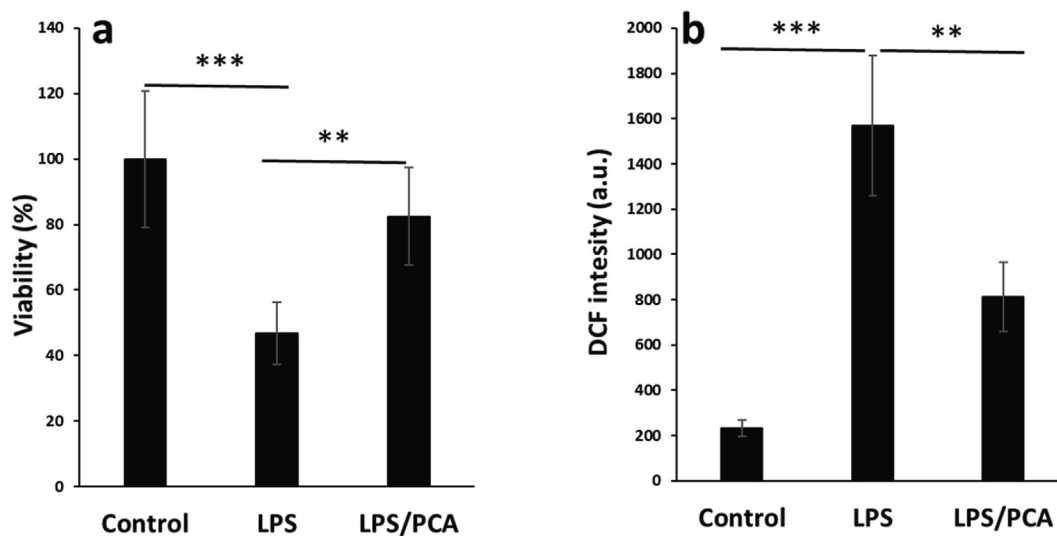


**Fig. 8.** Effects of PCA on the cytotoxicity and ROS production induced by LPS in type II AECs. (a) MTT assay, (b) ROS assay. The cells were treated with LPS (10  $\mu\text{g}/\text{mL}$ ) or co-incubated with LPS (10  $\mu\text{g}/\text{mL}$ ) and PCA (20  $\mu\text{M}$ ) for 24 h. Data are presented as mean  $\pm$  SD. \*\* $P < 0.01$ , \*\*\* $P < 0.001$  in comparison with the control group.

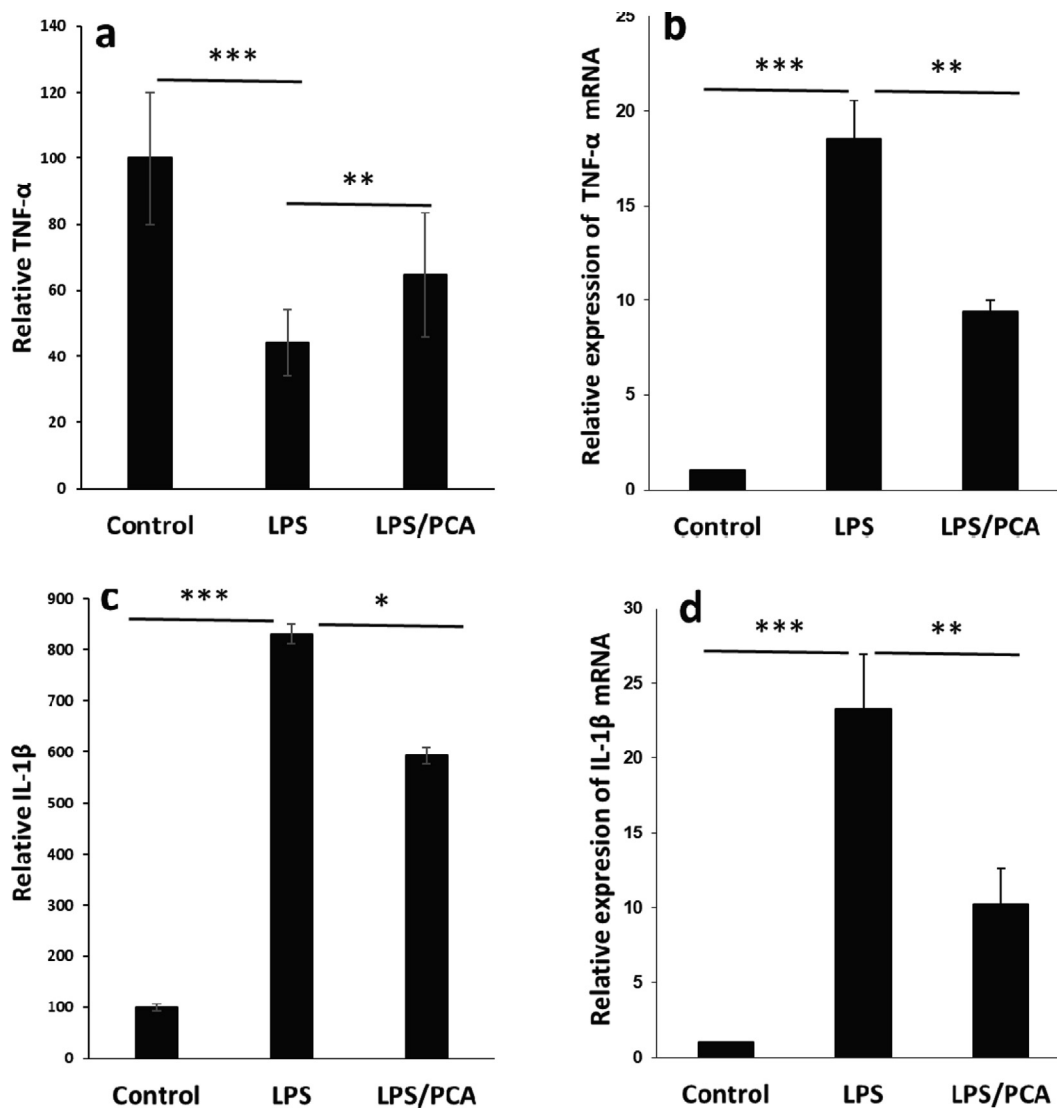


**Fig. 9.** Effects of PCA on the release and expression of pro-inflammatory mediators induced by LPS in type II AECs. (a) Relative TNF- $\alpha$  release assessed by ELISA assay, (b) Relative TNF- $\alpha$  mRNA expression assessed by real-time PCR assay, (c) Relative IL-1 $\beta$  release assessed by ELISA assay, (d) Relative IL-1 $\beta$  mRNA expression assessed by real-time PCR assay. The cells were treated with LPS (10  $\mu\text{g}/\text{mL}$ ) or co-incubated with LPS (10  $\mu\text{g}/\text{mL}$ ) and PCA (20  $\mu\text{M}$ ) for 24 h. Data are presented as mean  $\pm$  SD. \* $P < 0.05$ , \*\* $P < 0.01$ , \*\*\* $P < 0.001$  in comparison with the control group.

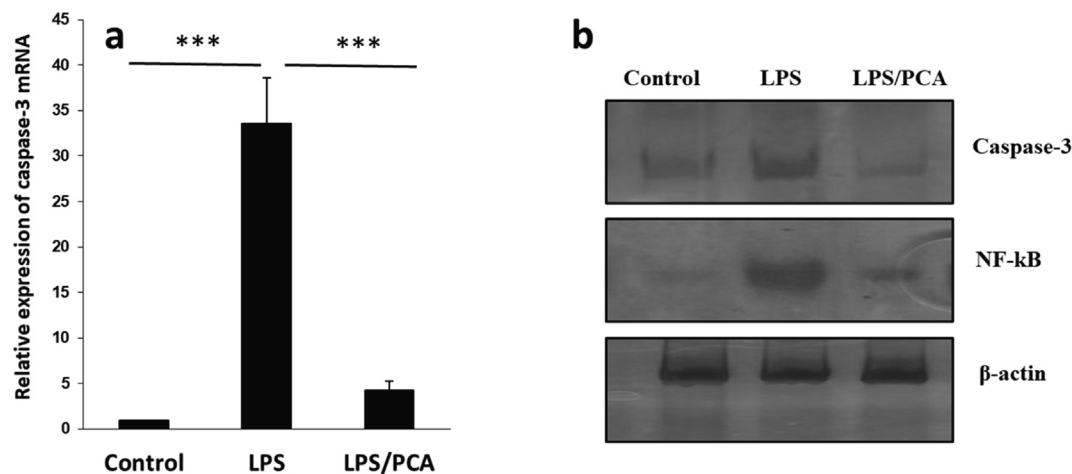


**Fig. 10.** (a) Effects of PCA on the expression of caspase-3 mRNA induced by LPS in type II AECs. (b) Western blot assay for the expression of caspase-3 and NF-κB. The cells were treated with LPS (10 μg/mL) or co-incubated with LPS (10 μg/mL) and PCA (20 μM) for 24 h. Data are presented as mean ± SD. \*\*\*P < 0.001 in comparison with the control group.

LPS and PCA (20 μM) regulated the reduction in cell viability induced by LPS and recovered the percentage of cell viability to 82.48%±14.91% (\*\*P < 0.01) (Fig. 8a). This data indicated that PCA can mitigate the triggered cytotoxicity by LPS in AECs.

It was also shown that incubation of cells with LPS resulted in a significant increase in the ROS production (\*\*\*\*P < 0.001), whereas the co-incubation of AECs with LPS and PCA reduced the production of ROS evidenced by DCF intensity (Fig. 8b). This data clearly showed that PCA may modulate the LPS-induced cytotoxicity in AEC cells through the regulation of ROS production (Zhang et al. 2021).

### 3.9. PCA decreased LPS-induced release and expression of pro-inflammatory cytokines in AECs

The present study indicated the protective potency of PCA against the ROS production induced by LPS in AECs. We detected that LPS induced cell toxicity by inducing oxidative stress production which was accompanied by an elevation in the level of ROS. In addition, it was found that the expression and the amount of pro-inflammatory cytokines such as TNF-α and IL-1β, were high in the AECs treated with LPS.

It was seen that LPS (10 μg/ml) exposure for 24 h induced the release and overexpression of pro-inflammatory cytokines, such as TNF-α (Fig. 9a, b) and IL-1β (Fig. 9c, d), which could induce the activation of the inflammatory response and apoptosis. TNF is known as a pleiotropic pro-inflammatory cytokine whose activation results in the expression of several pro-inflammatory cytokines, especially IL-1β (Reuter et al. 2010; Shahcheraghi et al. 2023). In the current report, LPS incubation led to a large release of TNF-α and IL-1β (Fig. 9a, c), and the mRNA expression levels of these markers were also elevated (Fig. 9b, d). This data indicated that LPS exposure triggered the expression of pro-inflammatory-associated markers and genes in AECs, and triggered an inflammatory response. However, this study reported that PCA affected the release of TNF-α and IL-1β, as well as the expression levels of TNF-α and IL-1β genes, revealing that PCA could relieve the side effects in inflammatory response induced by LPS stress.

### 3.10. PCA mitigated LPS-induced activation of apoptotic-related factor and NF-κB

It has been shown that LPS-induced cytotoxicity is derived from the activation of apoptosis (Daldal et al. 2022; Fu et al. 2022). LPS-induced oxidative stress can result in the regulation of apoptotic signaling pathways. Based on the above facts, we explored the expres-

sion of caspase-3 at mRNA and protein levels. It was seen that PCA mitigated the expression of caspase-3 mRNA (Fig. 10a) and caspase-3 protein (Fig. 10b) triggered by LPS exposure as evidenced by real-time PCR and western blot analysis, respectively. LPS treatment markedly elevated the level of caspase-3 mRNA and protein, while co-incubation of AECs with LPS and PCA resulted in a significant reduction in the protein and mRNA level of caspase-3. Also, PCA as an antioxidant, can be involved in regulating the cytotoxicity induced by LPS through inactivation of the NF-κB signaling pathways (Zhang et al. 2015). The NF-κB activation is involved in overexpression of pro-inflammatory signaling pathways (Roberti et al. 2022). Wang et al. reported that PCA could inhibit the expression of inflammatory mediators in LPS-triggered BV2 microglia via modulation of NF-κB and MAPK signaling pathways (Wang et al. 2015). Also, this study reported that PCA affects the expression level of NF-κB protein in LPS-treated cells, revealing that PCA could decrease the inflammatory response stimulated by LPS (Fig. 10b).

## 4. Conclusions

The interaction of PCA with an important plasma protein, HSA, was evaluated using spectroscopic and computational analyses. Also, the antioxidant properties of PCA against LPS-induced cytotoxicity and ROS production were assessed by different cellular and molecular assays. The motivation of this study was to investigate the interaction of a potential antioxidant bioactive compound, PCA, with HSA and also reveal the antioxidant signaling pathway regulated by PCA. It was shown that PCA strongly interacted with HSA based on a static quenching mechanism, and the interaction was mediated by the dominance of hydrophobic bonds. PCA partially increased the percentage of α-helix content of HSA as well as *Tm* of protein. PCA at the interacting site of HSA interacted with some hydrophobic amino acid residues. Also, PCA mitigated LPS-induced cytotoxicity in AECs through the reduction of ROS, and expression of pro-inflammatory and pro-apoptosis mediators mediated by inactivating the NF-κB signaling pathway. In conclusion, it can be deduced that PCA interacts strongly with HSA and shows antioxidant potential, which needs further investigations in future studies.

## Declaration of Competing Interest

The authors declare that they have no known competing financial interests or personal relationships that could have appeared to influence the work reported in this paper.

## References

- Abdelrahman, R.S., El-Tanbouly, G.S., 2022. Protocatechuic acid protects against thioacetamide-induced chronic liver injury and encephalopathy in mice via modulating mTOR, p53 and the IL-6/IL-17/IL-23 immunoinflammatory pathway. *Toxicol. Appl. Pharmacol.* 1, (440) 115931.
- Allenmark, S., Bomgren, B., Andersson, S., 1984. Some applications of chiral liquid affinity chromatography using bovine serum albumin as a stationary phase. *Prep. Biochem. Biotech.* 14 (2), 139–147.
- Aricov, L., Angelescu, D.G., Băran, A., Leontieș, A.R., Popa, V.T., Precupaș, A., Sandu, R., Sfîngă, G., Anghel, D.F., 2020. Interaction of piroxicam with bovine serum albumin investigated by spectroscopic, calorimetric and computational molecular methods. *J. Biomol. Struct. Dyn.* 38 (9), 2659–2671.
- Barnes, P.J., 2022. Oxidative stress in chronic obstructive pulmonary disease. *Antioxidants* 11 (5), 965.
- Bose, A., 2016. Interaction of tea polyphenols with serum albumins: A fluorescence spectroscopic analysis. *J. Lumin.* 1 (169), 220–226.
- Chamani, J., Moosavi-Movahedi, A.A., Hakimelahi, G.H., 2005. Structural changes in  $\beta$ -lactoglobulin by conjugation with three different kinds of carboxymethyl cyclodextrins. *Thermochim. Acta* 432 (1), 106–111.
- Dailah, H.G., 2022. Therapeutic potential of small molecules targeting oxidative stress in the treatment of chronic obstructive pulmonary disease (COPD): A comprehensive review. *Molecules* 27 (17), 5542.
- Daldal, H., Nazıroğlu, M., 2022. Rituximab attenuated lipopolysaccharide-induced oxidative cytotoxicity, apoptosis, and inflammation in the human retina cells via modulating the TRPM2 signaling pathways. *Ocul. Immunol. Inflamm.* 30 (6), 1315–1328.
- Eskew, M.W., Koslen, M.M., Benight, A.S., 2021. Ligand binding to natural and modified human serum albumin. *Anal. Biochem.* 1, (612) 113843.
- Farajzadeh-Dehkordi, N., Farhadian, S., Zahraei, Z., Asgharzadeh, S., Shareghi, B., Shakerian, B., 2023. Insights into the binding interaction of Reactive Yellow 145 with human serum albumin from a biophysics point of view. *J. Mol. Liq.* 1, (369) 120800.
- Faridbod, F., Ganjali, M.R., Larijani, B., Riahi, S., Saboury, A.A., Hosseini, M., Norouzi, P., Pillip, C., 2011. Interaction study of pioglitazone with albumin by fluorescence spectroscopy and molecular docking. *Spectrochim. Acta A Mol. Biomol. Spectrosc.* 78 (1), 96–101.
- Forsthuber, M., Kaiser, A.M., Granitzer, S., Hassl, I., Hengstschläger, M., Stangl, H., Gundacker, C., 2020. Albumin is the major carrier protein for PFOS, PFOA, PFHxS, PFNA and PFDA in human plasma. *Environ. Int.* 1, (137) 105324.
- Fu, Y., Jin, Y., Tian, Y., Yu, H., Wang, R., Qi, H., Feng, B., Zhang, J., 2022. Zearelanone promotes LPS-induced oxidative stress, endoplasmic reticulum stress, and accelerates bovine mammary epithelial cell apoptosis. *Int. J. Mol. Sci.* 23 (18), 10925.
- İlleriturk, M., Kandemir, O., Kandemir, F.M., 2022. Evaluation of protective effects of quercetin against cypermethrin-induced lung toxicity in rats via oxidative stress, inflammation, apoptosis, autophagy, and endoplasmic reticulum stress pathway. *Environ. Toxicol.* 37 (11), 2639–2650.
- Jiang SQ, Chen ZL, Zhang S, Ye JL, Wang YB. Protective effects of protocatechuic acid on growth performance, intestinal barrier and antioxidant capacity in broilers challenged with lipopolysaccharide. *animal*. 2023 Jan 1;17(1):100693.
- Jiang, Y., Wang, X., Yang, W., Gui, S., 2020. Procyanidin B2 suppresses lipopolysaccharides-induced inflammation and apoptosis in human type II alveolar epithelial cells and lung fibroblasts. *J. Interferon Cytokine Res.* 40 (1), 54–63.
- Kabir, M.Z., Tayyab, H., Erkmen, C., Kurbanoglu, S., Mohamad, S.B., Bengi, U.S., 2023. Characterization of Climbazole-Bovine serum albumin interaction by experimental and in silico approaches. *Spectrochim. Acta A Mol. Biomol. Spectrosc.* 5, (288) 122197.
- Kassab, R.B., Theyab, A., Al-Ghamdy, A.O., Algahtani, M., Mufti, A.H., Alsharif, K.F., Abdella, E.M., Habotta, O.A., Omran, M.M., Lokman, M.S., Bauomy, A.A., 2022. Protocatechuic acid abrogates oxidative insults, inflammation, and apoptosis in liver and kidney associated with monosodium glutamate intoxication in rats. *Environ. Sci. Pollut. Res.* 1, 1–4.
- Khan, H., Grewal, A.K., Singh, T.G., 2022. Pharmacological postconditioning by protocatechuic acid attenuates brain injury in ischemia-reperfusion (I/R) mice model: Implications of nuclear factor erythroid-2-related factor pathway. *Neuroscience* 21 (491), 23–31.
- Khashkhashi-Moghadam, S., Ezazi-Toroghi, S., Kamkar-Vatanparast, M., Jouyaeian, P., Mokaberi, P., Yazdyani, H., Amiri-Tehrani-zadeh, Z., Saberi, M.R., Chamani, J., 2022. Novel perspective into the interaction behavior study of the cyanidin with human serum albumin-holo transferrin complex: Spectroscopic, calorimetric and molecular modeling approaches. *J. Mol. Liq.* 15, (356) 119042.
- Kratz, F., 2014. A clinical update of using albumin as a drug vehicle—A commentary. *J. Control. Release* 28 (190), 331–336.
- Lee, W.J., Lee, S.H., 2022. Protocatechuic acid protects hepatocytes against hydrogen peroxide-induced oxidative stress. *Curr. Res. Food Sci.* 1 (5), 222–227.
- Liang, J., Zhang, K., Li, J., Su, J., Guan, F., Li, J., 2022. Injectable protocatechuic acid based composite hydrogel with hemostatic and antioxidant properties for skin regeneration. *Mater. Des.* 1, (222) 111109.
- Merlino, A., 2023. Metalloprotein binding to serum albumin: Lessons from biophysical and structural studies. *Coord. Chem. Rev.* 1, (480) 215026.
- Mert, H., Kerem, Ö., Mis, L., Yildirim, S., Mert, N., 2022. Effects of protocatechuic acid against cisplatin-induced neurotoxicity in rat brains: an experimental study. *Int. J. Neurosci.* 16, 1.
- Mostafavi, E.S., Asoodeh, A., Chamani, J., 2022. Evaluation of interaction between Ponceau 4R (P4R) and trypsin using kinetic, spectroscopic, and molecular dynamics simulation methods. *J. Mol. Liq.* 15, (362) 119761.
- Naik, R., Seetharamappa, J., 2022. Elucidating the binding mechanism of an antimigraine agent with a model protein: insights from molecular spectroscopic, calorimetric and computational approaches. *J. Biomol. Struct. Dyn.* 14, 1–6.
- Negrea, E., Oancea, P., Leonties, A., Maria, U.A., Avram, S., Raducan, A., 2023. Spectroscopic studies on binding of ibuprofen and drotaverine with bovine serum albumin. *J. Photochem. Photobiol. A Chem.* 1, (438) 114512.
- Nwozo, O.S., Effiong, E.M., Aja, P.M., Awuchi, C.G., 2023. Antioxidant, phytochemical, and therapeutic properties of medicinal plants: a review. *Int. J. Food Prop.* 26 (1), 359–388.
- Osman, M.M., El-Shaheny, R., Ibrahim, F.A., 2023. Perception of the interaction behavior between pepsin and the antimicrobial drug secnidazole with combined experimental spectroscopy and computer-aided techniques. *Spectrochim. Acta A Mol. Biomol. Spectrosc.* 9, 122336.
- Parham, S., Kharazi, A.Z., Bakhsheshi-Rad, H.R., Nur, H., Ismail, A.F., Sharif, S., RamaKrishna, S., Berto, F., 2020. Antioxidant, antimicrobial and antiviral properties of herbal materials. *Antioxidants* 9 (12), 1309.
- Rao, H., Qi, W., Su, R., He, Z., Peng, X., 2020. Mechanistic and conformational studies on the interaction of human serum albumin with rhodamine B by NMR, spectroscopic and molecular modeling methods. *J. Mol. Liq.* 10, (316) 113889.
- Reuter, S., Gupta, S.C., Chaturvedi, M.M., Aggarwal, B.B., 2010. Oxidative stress, inflammation, and cancer: how are they linked? *Free Radic. Biol. Med.* 49 (11), 1603–1616.
- Rizzuti, B., Bartucci, R., Pey, A.L., Guzzi, R., 2019. Warfarin increases thermal resistance of albumin through stabilization of the protein lobe that includes its binding site. *Arch. Biochem. Biophys.* 15, (676) 108123.
- Roberti, A., Chaffey, L.E., Greaves, D.R., 2022. NF- $\kappa$ B signaling and inflammation—Drug repurposing to treat inflammatory disorders? *Biology* 11 (3), 372.
- Sarzehi, S., Chamani, J., 2010. Investigation on the interaction between tamoxifen and human holo-transferrin: determination of the binding mechanism by fluorescence quenching, resonance light scattering and circular dichroism methods. *Int. J. Biol. Macromol.* 47 (4), 558–569.
- Shahcheraghi, S.H., Salemi, F., Small, S., Syed, S., Salari, F., Alam, W., Cheang, W.S., Saso, L., Khan, H., 2023. Resveratrol regulates inflammation and improves oxidative stress via Nrf2 signaling pathway: Therapeutic and biotechnological prospects. *Phytother. Res.*
- Siddiqui S, Ameen F, ur Rehman S, Sarwar T, Tabish M. Studying the interaction of drug/ligand with serum albumin. *Journal of Molecular Liquids*. 2021 Aug 15;336:116200.
- Song, Y., Niu, Y., Zheng, H., Yao, Y., 2021. Interaction of Bis-guanidinium acetates surfactants with bovine serum albumin evaluated by spectroscopy. *Tenside Surfactant Deterg.* 58 (3), 187–194.
- Stolz, D., Mkorombindo, T., Schumann, D.M., Agusti, A., Ash, S.Y., Bafadhel, M., Bai, C., Chalmers, J.D., Criner, G.J., Dharmage, S.C., Franssen, F.M., 2022. Towards the elimination of chronic obstructive pulmonary disease: a Lancet Commission. *Lancet* 400 (10356), 921–972.
- Varshney, A., Sen, P., Ahmad, E., Rehan, M., Subbarao, N., Khan, R.H., 2010. Ligand binding strategies of human serum albumin: how can the cargo be utilized? *Chirality: Pharmacol. Biol. Chem. Consequences Mol. Asymmetry* 22 (1), 77–87.
- Vuong, T.V., 2021. Natural products and their derivatives with antibacterial, antioxidant and anticancer activities. *Antibiotics* 10 (1), 70.
- Wang L, Liang YS, Wu ZB, Liu YS, Xiao YH, Hu T, Gao R, Fang J, Liu J, ping Wu A. Exploring the interaction between Cry1Ac protein and Zn<sup>2+</sup>, Cd<sup>2+</sup> metal ions by fluorescence quenching and molecular docking approaches. *Chemosphere*. 2022 Jun 1;297:134105.
- Wang, H.Y., Wang, H., Wang, J.H., Wang, Q., Ma, Q.F., Chen, Y.Y., 2015. Protocatechuic acid inhibits inflammatory responses in LPS-stimulated BV2 microglia via NF- $\kappa$ B and MAPKs signaling pathways. *Neurochem. Res.* 40, 1655–1660.
- Yeggoni, D.P., Meti, M., Subramanyam, R., 2022. Chebulinic and chebulagic acid binding with serum proteins: biophysical and molecular docking approach. *J. Biomol. Struct. Dyn.* 1, 1–6.
- Yesildag, K., Gur, C., İlleriturk, M., Kandemir, F.M., 2022. Evaluation of oxidative stress, inflammation, apoptosis, oxidative DNA damage and metalloproteinases in the lungs of rats treated with cadmium and carvacrol. *Mol. Biol. Rep.* 49 (2), 1201–1211.
- Yu L, Hua Z, Luo X, Zhao T, Liu Y. Systematic interaction of plasma albumin with the efficacy of chemotherapeutic drugs. *Biochimica et Biophysica Acta (BBA)-Reviews on Cancer*. 2022 Jan 1;1877(1):188655.
- Zhang, S., Gai, Z., Gui, T., Chen, J., Chen, Q., Li, Y., 2021. Antioxidant effects of protocatechuic acid and protocatechuic aldehyde: old wine in a new bottle. *Evid. Based Complement. Alternat. Med.* 8, 2021.
- Zhang, X., Li, C., Li, J., Xu, Y., Guan, S., Zhao, M., 2015. Protective effects of protocatechuic acid on acute lung injury induced by lipopolysaccharide in mice via p38MAPK and NF- $\kappa$ B signal pathways. *Int. Immunopharmacol.* 26 (1), 229–236.
- Zhou, C., Xu, R., Han, X., Tong, L., Xiong, L., Liang, J., Sun, Y., Zhang, X., Fan, Y., 2023. Protocatechuic acid-mediated injectable antioxidant hydrogels facilitate wound healing. *Compos. B Eng.* 1, (250) 110451.